Genomic Alterations in Human Papillomavirus–Positive and –Negative Conjunctival Squamous Cell Carcinomas

Ingvild Ramberg,[1,2] Filipe Garrett Vieira,[3] Peter Bjerre Toft,[1,4] Christian von Buchwald,[4,5] Mikkel Funding,[6] Finn Cilius Nielsen,[3] and Steffen Heegaard[1,2,4]

[1]Department of Ophthalmology, Copenhagen University Hospital Rigshospitalet, Copenhagen, Denmark
[2]Department of Pathology, Copenhagen University Hospital Rigshospitalet, Copenhagen, Denmark
[3]Center for Genomic Medicine, Rigshospitalet, University of Copenhagen, Copenhagen, Denmark
[4]Department of Clinical Medicine, Copenhagen University, Copenhagen, Denmark
[5]Department of Otorhinolaryngology, Head and Neck Surgery, and Audiology, Copenhagen University Hospital Rigshospitalet, Copenhagen, Denmark
[6]Department of Ophthalmology, Aarhus University Hospital, Aarhus, Denmark

Correspondence: Steffen Heegaard, Department of Pathology, Copenhagen University Hospital Rigshospitalet Denmark, Department of Ophthalmology, Copenhagen University Hospital Rigshospitalet, Denmark; sthe@sund.ku.dk.

Received: April 12, 2021
Accepted: October 14, 2021
Published: November 15, 2021

Citation: Ramberg I, Vieira FG, Toft PB, et al. Genomic alterations in human papillomavirus–positive and –negative conjunctival squamous cell carcinomas. *Invest Ophthalmol Vis Sci.* 2021;62(14):11. https://doi.org/10.1167/iovs.62.14.11

Purpose. The genomic alterations contributing to the pathogenesis of conjunctival squamous cell carcinomas (SCCs) and their precursor lesions are poorly understood and hamper our ability to develop molecular therapies to reduce the recurrence rates and treatment-related morbidities of this disease. We aimed to characterize the somatic DNA alterations in human papillomavirus (HPV)–positive and HPV-negative conjunctival SCC.

Methods. Patients diagnosed with conjunctival SCC in situ or SCC treated in ocular oncology referral centers in Denmark were included. HPV detection (HPV DNA PCR, p16 immunohistochemistry, and mRNA in situ hybridization) and targeted capture-based next-generation sequencing of 523 genes frequently involved in cancer were performed to describe the mutational profile based on HPV status.

Results. Tumor tissue was available in 33 cases ($n = 8$ conjunctival SCCs in situ, $n = 25$ conjunctival SCCs), constituting 25 male and 8 female patients. Nine cases were HPV positive. The HPV-positive SCCs in situ and SCCs were characterized by transcriptionally active high-risk HPV (types 16 and 39) within the tumor cells, frequent mutations in *PIK3CA* ($n = 5/9$), and wild-type *TP53*, *CDKN2A*, and *RB1*, while the HPV-negative counterparts harbored frequent mutations in *TP53* ($n = 21/24$), *CDKN2A* ($n = 7/24$), and *RB1* ($n = 6/24$).

Conclusions. Our findings have delineated two potentially distinct distributions of somatic mutations in conjunctival SCC based on HPV status—pointing to different biological mechanisms of carcinogenesis. The present findings support a causal role of HPV in a subset of conjunctival SCC.

Keywords: conjunctiva, human papillomavirus, next-generation sequencing, carcinoma

Conjunctival squamous cell carcinoma (SCC) is the most frequent malignancy of the conjunctiva worldwide, and the incidence is increasing.[1,2] Although conjunctival SCC is traditionally considered a low-risk malignancy, approximately 10% of the cases require orbital exenteration due to invasive orbital disease.[3,4] Furthermore, recurrence rates are reported in up to 56%.[5,6] Large series have shown an overall survival rate of 70% after 5 years and 50% years after 10 years, which is similar to patients with conjunctival malignant melanoma.[7]

Primary surgical excision followed by adjunctive cryotherapy of the conjunctival margins forms the mainstay of treatment. Some institutions also apply topical or intralesional chemotherapy, such as mitomycin C, interferon α2b, or 5-fluorouracil, as monotherapy or chemoreduction of large lesions or radiotherapy. However, nonresponsiveness to topical chemotherapy is a clinical challenge.[8–10] Moreover, consensus regarding adjuvant therapy and treatment regimens of advanced and recurrent disease is lacking. These challenges are partly due to our poor understanding of the underlying genomic mechanisms that cause and drive disease development, hampering our ability to develop molecular therapies to reduce the recurrence rates and treatment-related morbidities.

Exposure to UV radiation is considered the main risk factor for developing conjunctival SCC; however, there is also emerging evidence of high-risk human papillomavirus (HPV) as an important contributor to the disease development.[11] In other anatomic sites, such as the oropharynx, the clinical and histologic profile of HPV-related SCC differs from the HPV-unrelated counterparts. This is mirrored in the affection of distinct intracellular pathways and thereby creating the potential for differentiated treatment regimens based on HPV status.[12,13]

The present study aimed to further our understanding of the contribution of somatic genomic alterations in the pathogenesis of HPV-positive and HPV-negative conjunctival SCC by DNA sequencing of 523 genes frequently altered in cancer.

Materials and Methods

This retrospective case series was prospectively approved by the Danish Data Protection Agency (Journal no: RH-2013-30-1035, 02288) and the Regional Scientific Ethics Committee of the Capital Region of Denmark (Journal no: H-16044879, 55827), and it was conducted according to the Declaration of Helsinki.

Tissue Samples

We included patients with a histopathologic diagnosis of a treatment-naive, primary conjunctival squamous cell carcinoma or carcinoma in situ diagnosed in Denmark between 1995 and 2019 by searching the Danish Pathology Register. The registry has had a national coverage of almost 100% since 1997,[14] when it became a legal obligation to register all surgical pathology specimens in the database, although it contains data from 1970. To detect cases not submitted to the Danish Pathology Register, we manually reviewed the pathology records at the Eye Pathology Section, Copenhagen University Hospital, Rigshospitalet, Denmark, which has ophthalmic pathology expertise and receives samples from private ophthalmologists and hospitals all over Denmark. A total of 76 patients were identified in the database searches. The corresponding medical files were retrieved when available and clinical data (including age at diagnosis, gender, size and location of the tumor, and treatment) were extracted. The formalin-fixed, paraffin-embedded (FFPE) tumor tissue blocks were retrieved from the pathology departments all over Denmark. The histopathologic diagnosis was validated from a hematoxylin and eosin (HE)–stained section of each tumor and staged according to the eighth edition of the American Joint Commission on Cancer staging manual by an ophthalmic pathologist (SH).[15] FFPE blocks with no or limited tumor tissue were considered unsuitable for ancillary molecular testing and thereby excluded. The samples were macroscopically dissected guided by an HE slide to separate tumor tissue from surrounding normal stromal tissue and areas of necrosis to enrich the amount of tumor DNA for further analyses (Fig. 1). After validation of the diagnosis, the following procedure was followed: sections for DNA extraction, sections for immunohistochemistry, and eventually sections for in situ hybridization. Six to eight FFPE sections per tumor block were used for DNA extraction. Tumor DNA was isolated using the Gene Read DNA FFPE kit (#180134; Qiagen, Hilden, Germany) on QIAcube (Qiagen). The kit removes deaminated cytosine residues from DNA extracted from FFPE to minimize FFPE-induced cytosine-to-thymine conversion artifacts in the downstream analyses.[16] Quantification of purified DNA was performed using the Qubit DNA HS assay kit (Life Technologies Invitrogen, Thermo Fisher Scientific, Waltham, MA, USA). Samples with a DNA level below 250 ng were excluded. A total of 33 cases met the inclusion criteria and were included in the study.

Detection of Human Papillomavirus

HPV detection was performed by HPV DNA PCR, p16 immunohistochemistry (IHC), and E6/E7 mRNA in situ hybridization (ISH) as described in the following sections.

HPV and GAPDH DNA PCR. To ensure DNA integrity, a PCR of the housekeeping gene GAPDH using the GAPDH-a/GAPDH-b primers was performed in all cases. PCR for detection for HPV DNA was performed using the general primers GP5+/6+ (5′TTTGTTACTGTGGTAGATACTAC3′ and 5′GAAAAATAAACTGTAAATCATATTC3′) targeting the L1 region of the HPV genome. The expected amplicon sizes

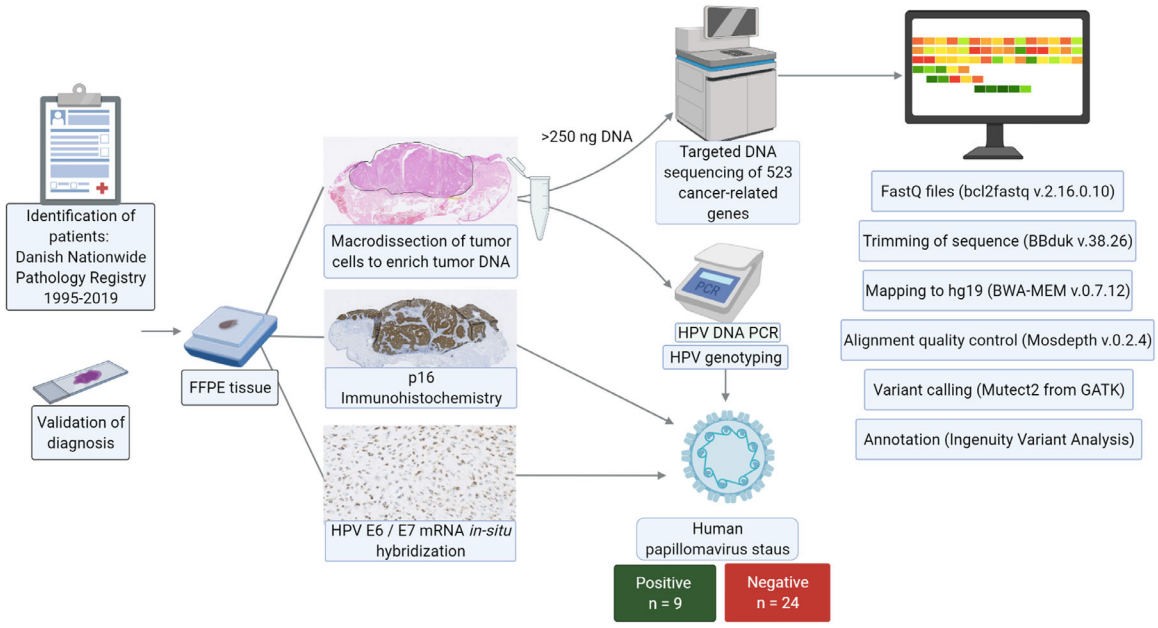

Figure 1. The workflow from sample retrieval of FFPE tissue to multimodal HPV testing and targeted DNA sequencing of 523 cancer-related genes. HPV positivity was defined as positive results in HPV DNA PCR, mRNA ISH, and p16 immunohistochemistry. The figure was created using BioRender.com.

Investigative Ophthalmology & Visual Science

were 150 base pairs for the GP5+/6+ primers and 200 base pairs for GAPDH. The amplicons were resolved on a 2.5% agarose gel and stained with ethidium bromide. Negative (H_2O) and positive controls (pool of HPV-positive tumors) were included in each case.

HPV Genotyping. HPV genotyping was performed by sequencing using the KAPA HTP Library Preparation Kit (Kapabiosystems; Roche Diagnostics Basel, Switzerland) for library construction. The indexed adaptors (NEXTflex-96 DNA Barcodes; Bioo Scientific Austin, TX, USA) were ligated and end-repaired. The quality of the purified library was evaluated using the High Sensitivity D5000 kit (Agilent Technology Santa Clara, CA, USA) by automated electrophoresis (TapeStation; Agilent). The quantity was evaluated using the Qubit dsDNA BR Kit on a Qubit Fluorometer (Invitrogen, Thermo Fisher Scientific, Waltham MA, USA). Paired-end, multiplex sequencing was performed on a MiSeq (Illumina, San Diego CA, USA). The reads were mapped to reference genomes for HPV (HPV_REF, downloaded from the papillomavirus database "PaVe" at https://pave.niaid.nih.gov/).

P16INK4a Immunohistochemistry. The 4-µm paraffin sections were evaluated for p16 expression. Immunohistochemistry was performed on the automated immunostainer Ventana BenchMark Ultra (Roche, Ventana Medical Systems, Roche, Oro Valley, AZ, USA) using the UltraView/Optiview detection kit (760-500/760-700) following the manufacturer's immunohistochemistry staining protocol. The slides were incubated with the monoclonal mouse anti-p16 antibody (clone E6H4; Roche Diagnostics), counterstained with hematoxylin II and bluing reagent, and mounted under coverslips. Positive and negative controls were employed for all sections. A strong and diffuse nuclear and cytoplasmic staining in more than 75% of the tumor cells was considered p16 positive.

mRNA In Situ Hybridization. In situ hybridization to detect the HPV oncogenes E6 and E7 mRNA was performed on 6-µm paraffin sections using an automated staining system (Ventana Discovery ULTRA staining module; Ventana Medical Systems). The cutting of slides was performed <24 hours before staining to ensure the best possible integrity of the RNA. The RNA integrity was evaluated by running the analysis with the housekeeping gene cyclophilin B (PPIB) as a positive control prior to hybridization with the HPV probe and in each subsequent run. We used the bacterial gene dapB (diaminopimelate B) as a negative control to determine if the tissue specimen was appropriately prepared for the analysis. The DapB control slides determined nonspecific staining. We used the automated RNAscope VS Reagent Kit (Advanced Cell Diagnostics, Newark CA, USA) with the HPV18 cocktail probe (for detection of the high-risk strains HPV 16, 18, 26, 31, 33, 35, 39, 45, 51, 52, 53, 56, 58, 59, 66, 68, 73, and 82; cat. 312598, Advanced Cell Diagnostics). The sections were deparaffinized, underwent proteolytic digestion with enzyme denaturation, and were incubated with the HPV cocktail probe according to the manufacturer's protocol. The sections were counterstained with hematoxylin II and bluing agent. All stains were scored semiquantitively according to the RNAscope Assay scoring guidelines (grade 0: no staining or <1 dot per 10 cells; grade 1: 1–3 dots per cell; grade 2: 4–9 dots per cell; grade 3: 10–15 dots per cell and <10% of dots were in clusters; grade 4: >15 dots/cell and >10% of dots were in clusters). One dot corresponds to a single copy of an mRNA molecule. Overall, HPV positivity was defined as a positive HPV DNA PCR, grade ≥1 in mRNA ISH, and >75% diffuse and nuclear staining in p16 IHC.

Library Preparation and DNA Sequencing

Samples with a sufficient quantity of DNA (minimum input DNA was set to 250 ng) was available in 33 out of the 76 cases. Library preparation was performed using the hybrid-capture TruSight Oncology 500 Library Preparation Kit (Illumina), targeting 523 frequently altered genes in cancer (Supplementary Material). We followed the TruSight Oncology 500 Reference Guide from Illumina (Document no: 1000000067621; https://support.illumina.com/downloads/trusight-oncology-500-reference-guide-1000000067621.html). Libraries were sequenced on a NovaSeq 6000 (Illumina) for 2 × 150-bp paired-end reads according to the manufacturer's protocol.

Bioinformatic Analysis

Initially, the raw sequencing files (.bcl files) were converted to individual FASTQ files using the bcl2fastq v2.16.0.10 (Illumina). A read quality assessment was performed for each sequencing library using FastQC version 0.11.85.[17] All 33 samples had sufficient quality to be included in the downstream analyses. Then, the sequenced reads were trimmed to remove technical sequences (e.g., sequencing adaptors and low-quality ends with BBduk version 38.26). The reads were mapped to the human hg19/GRCh37 reference genome using BWA-MEM version 0.7.12. An alignment quality assessment was performed with the command-line tool Mosdepth version 0.2.4 to calculate coverage across the regions of interest.[18] The variant calling was performed with Mutect2 from the Genome Analysis Toolkit (GATK) (Broad Institute, Cambridge MA, USA) package (version 4.1.0.0) following GATK's best practices for somatic short variant discovery.[19] As we did not have a matched normal sample or a panel of normal samples, we performed somatic variant calling using only the Genome Aggregation Database version 2.1.1[20] as a germline resource, correcting for both read orientation and sample contamination.

Ingenuity Variant Analysis (Qiagen Bioinformatics, Redwood City, CA, USA) was used for customized variant annotations. The samples were filtered based on the following criteria: a call quality above 20, a read depth of at least 100, and a variant allele fraction of at least 0.10. Variants reported in the healthy public genomes (1000 Genomes Project), the Exome Sequencing Project, or the Exome Aggregation Consortium databases with a frequency >0.1 were considered germline variations and thereby excluded. Furthermore, the variant should be outside the top 5% of the most exonically variable 100 base windows in healthy public genomes and should pass the built-in upstream pipeline filtering in the Ingenuity software (variants classified with a PASS value in the variant call file) to help exclude spurious calls. Variants classified as "benign" or "likely benign" were excluded. Variants classified as "pathogenic," "likely pathogenic," or "uncertain" were looked up in the Catalogue of Somatic Mutations in Cancer database (cancer.sanger.ac.uk) and cBioPortal for Cancer Genomics (www.cbioportal.org).[21,22] Variants classified as "uncertain" in the upstream analysis and not previously reported in the cancer databases were not annotated. All annotated variants were visually inspected by the Integrative Genomics Viewer version 2.5.2. The variant call files were converted to mutation annotation files using vcf2maf and visualized using the R Bioconductor package Maftools version 3.13 and the MutationMapper on www.cBioportal.org.[21–23] Only variants classified as frameshift deletion, frameshift insertion, splice site, nonsense mutation,

nonstop mutation, inframe deletion, inframe insertion, or missense mutation were included in the illustrations, as others were assumed to be silent variants. The sequencing data are available in the European Variation Archive at https://www.ebi.ac.uk/eva/, reference number PRJEB47801 (study accession) ERZ3611730 (analysis accession).

Results

Tumor samples from 33 patients with primary, treatment-naive conjunctival SCC in situ ($n = 8$) and invasive conjunctival SCC ($n = 25$) were included in the study, constituting 8 female and 25 male patients with a median age at diagnosis of 70 years (range, 54–97 years) (Table). Ten patients had a tumor located in the inferior tarsal conjunctiva, while the rest were located in the bulbar conjunctiva, most often in the medial corneal limbus ($n = 9$).

Human Papillomavirus in Conjunctival SCC In Situ and SCC

Samples from nine patients were positive in HPV DNA PCR, E6/E7 mRNA ISH, and p16 IHC and thereby considered HPV positive ($n = 3$ SCCs in situ, $n = 6$ SCCs, Table). The detected genotypes were HPV 16 ($n = 8$) and HPV 39 ($n = 1$). One sample was HPV 16 positive by PCR but negative in p16 IHC and E6/E7 mRNA ISH and therefore considered HPV negative along with the remaining 23 samples that yielded negative results in HPV PCR and mRNA ISH (Supplementary Figure S1).

Targeted DNA Sequencing of 523 Cancer-Related Genes

The median sequencing coverage across all targeted bases was 770× (range, 346–1686×), with more than 98% of target reads above 50× coverage, enabling a sensitive mutation detection even in the presence of stromal cell contamination. Most mutations were missense mutations and nonsense mutations with enrichment of C>T transitions. A median of 3 (range, 2–9) and 6 (1–15) variants classified as likely driving oncogenic or tumor suppressor mutations per sample were detected in HPV-positive and HPV-negative tumors, respectively. An overview of the top 12 nonsynonymous mutated genes and the variant classification is provided in Figure 2a. A list of all annotated mutations is provided in the Supplementary Material. Overall, the most frequently encountered mutations were in *TP53* ($n = 22$; 67%), *KMT2D* ($n = 8$; 24%), *PIK3CA* ($n = 8$; 24%), *CDKN2A* ($n = 7$; 21%), and *RB1* ($n = 6$; 18%).

All mutations in *TP53* are considered pathogenic or likely pathogenic variants (p.X32_splice, p.S127P/F, p.P152L/S, p.G187_splice, p.C176Y, p.Q192*, p.R196*, p.R213*, p.K291E, P.Y220C, p.R248W, p.E258K, p.Q317*, p.C277del, p.R282W, p.E286K, p.R342*, p.R290C, and p.R273G), primarily affecting the DNA-binding domain of

Table. Clinicopathologic Characteristics of 33 Conjunctival Squamous Cell Carcinomas In Situ and Carcinomas in a Danish Cohort

Sample	Age (y), Sex	Diagnosis	AJCC Stage	Location	P16 IHC	HPV PCR	HPV Genotype	mRNA ISH	Affected Pathways
1	61, M	CIS	Tis	Medial limbus	Negative	Negative	Negative	Negative	TP53, PI3K
2	67, M	CIS	Tis	Medial limbus	Negative	Positive	HPV 16	Negative	Cell cycle, TP53, RTK-RAS
3	76, F	CIS	Tis	Bulbar conjunctiva	Positive	Negative	Negative	Negative	Cell cycle, TP53
4	87, M	CIS	Tis	Medial limbus	Negative	Negative	Negative	Negative	Hippo, TP53
5	97, M	CIS	Tis	Medial limbus	Positive	Negative	Negative	Negative	Cell cycle, NOTCH, PI3K
6	55, M	CIS	Tis	Medial limbus	Positive	Positive	HPV 39	Positive	TP53, PI3K
7	56, F	CIS	Tis	Bulbar conjunctiva	Positive	Positive	HPV 16	Positive	PI3K
8	74, M	CIS	Tis	NA	Positive	Positive	HPV 16	Positive	PI3K
9	60, M	SCC	T1N0M0	Medial limbus	Negative	Negative	Negative	Negative	Cell cycle, TP53
10	70, M	SCC	T1N0M0	Lateral limbus	Positive	Negative	Negative	Negative	Cell cycle, TP53, RTK-RAS
11	82, M	SCC	T1N0M0	Bulbar conjunctiva	Positive	Negative	Negative	Negative	TP53, NOTCH
12	54, F	SCC	T2N0M0	Tarsal conjunctiva	Positive	Negative	Negative	Negative	Cell cycle, TP53, PI3K
13	60, F	SCC	T2N0M0	Tarsal conjunctiva	Negative	Negative	Negative	Negative	TP53
14	62, M	SCC	T2N0M0	Tarsal conjunctiva	Negative	Negative	Negative	Negative	TP53
15	66, M	SCC	T2N0M0	Lateral limbus	Negative	Negative	Negative	Negative	Cell cycle, TP53, RTK-RAS
16	69, M	SCC	T2N0M0	Medial limbus	Positive	Negative	Negative	Negative	Cell cycle, NOTCH
17	87, M	SCC	T2N0M0	Bulbar conjunctiva	Negative	Negative	Negative	Negative	Cell cycle, TP53, PI3K
18	92, F	SCC	T2N0M0	Tarsal conjunctiva	Positive	Negative	Negative	Negative	Cell cycle, TP53, PI3K
19	92, M	SCC	T2N0M0	Lateral limbus	Negative	Negative	Negative	Negative	Cell cycle, TP53, RTK-RAS
20	61, F	SCC	T3N0M0	Tarsal conjunctiva	Negative	Negative	Negative	Negative	Cell cycle, TP53
21	62, M	SCC	T3N0M0	Diffuse	Negative	Negative	Negative	Negative	TP53, RTK-RAS, PI3K
22	82, M	SCC	T3N0M0	Tarsal conjunctiva	Negative	Negative	Negative	Negative	TP53
23	94, M	SCC	T3N0M0	Diffuse	Negative	Negative	Negative	Negative	TP53, RTK-RAS
24	81, M	SCC	T4N0M0	Tarsal conjunctiva	Negative	Negative	Negative	Negative	TP53, NOTCH, RTK-RAS
25	74, M	SCC	NA	Lateral limbus	Negative	Negative	Negative	Negative	TP53, RTK-RAS
26	75, M	SCC	NA	NA	Positive	Negative	Negative	Negative	Cell cycle, TP53, NOTCH
27	80, M	SCC	NA	Medial limbus	Negative	Negative	Negative	Negative	TP53
28	61, M	SCC	T1N0M0	Lateral limbus	Positive	Positive	HPV 16	Positive	Cell cycle, RTK-RAS
29	77, M	SCC	T1N0M0	Tarsal conjunctiva	Positive	Positive	HPV 16	Positive	RTK-RAS
30	62, M	SCC	T4N0M0	Medial limbus	Positive	Positive	HPV 16	Positive	PI3K
31	64, F	SCC	T4N0M0	Tarsal conjunctiva	Positive	Positive	HPV 16	Positive	RTK-RAS, PI3K
32	69, F	SCC	T4N0M0	Caruncle	Positive	Positive	HPV 16	Positive	TP53, RTK-RAS
33	71, M	SCC	T4N1M1	Tarsal conjunctiva	Positive	Positive	HPV 16	Positive	PI3K

The cell cycle pathway includes *CDKN2A*, *RB1*, and *CDK4*; the Hippo signaling pathway includes *GNAS*; the TP53 pathway includes *TP53* and *ATM*; the NOTCH pathway includes *CREBBP*, *NOTCH1*, *NOTCH3*, and *EP300*; the RTK-RAS pathway includes *FGFR1*, *FGFR3*, *MET*, *NF1*, *JAK2*, *NRAS*, *RASA1*, and *RET*; and the PI3K pathway includes *PIK3CA*, *TSC1*, *TSC2*, *MTOR*, *PPP2R1A*, and *STK11*. AJCC: American Joint Committee on Cancer; CIS, squamous cell carcinoma in situ; F, female; M, male; NA: Not applicable.

Investigative Ophthalmology & Visual Science

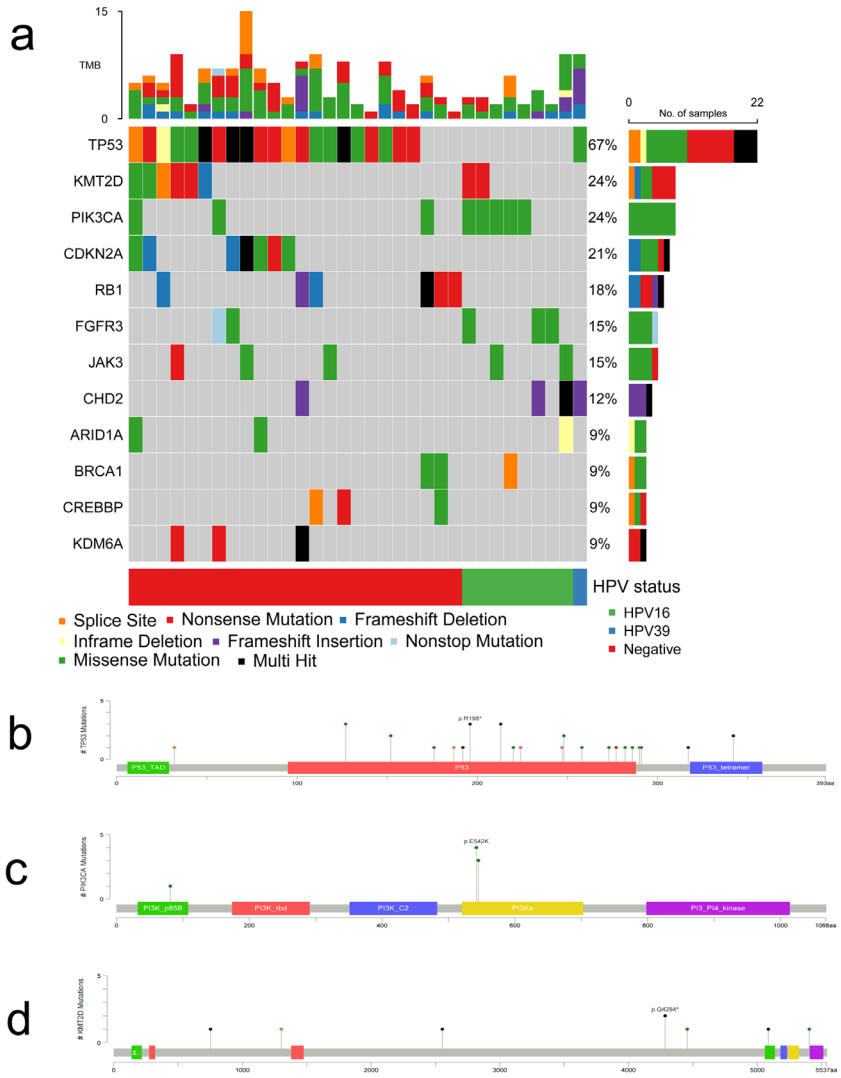

Figure 2. (**a**) A summary of the top 12 mutated genes in conjunctival SCC, sorted by HPV status. The rows represent the affected genes and the columns represent the different samples. *TP53* was the most frequently mutated gene in HPV-negative conjunctival SCC, whereas HPV-positive SCC most frequently harbored missense mutations in *PIK3CA* combined with wild-type status of *TP53*. (**b**) Annotated mutations in *TP53* primarily affecting the DNA-binding domain of p53. (**c**) Annotated mutations in *PIK3CA* primarily located in the helical domains. (**d**) Mutations in *KMT2D* were frequently reported in our series, enriched among invasive carcinoma samples.

the p53 protein (Fig. 2b). Four patients had multiple functionally relevant genomic alterations in *TP53*. All mutations in *PIK3CA* were missense mutations within hotspot regions of the gene with well-established activating downstream effects (p.E81K, p.E542K, and p.E545K) (Fig. 2c). Among the mutations in *KMT2D*, four variants have previously been described in the literature and are considered pathogenic (p.Q2553*, p.Q4284*, p.R5086*, and p.R5432Q) (Fig. 2d). Three novel likely pathogenic mutations in *KMT2D* were identified (p.L752Vfs*5, splice site loss p.X1303_splice, and p.S4456L). All mutations in *CDKN2A* were inactivating mutations previously reported in the literature (p.P48L, p.P114L, p.R80*, p.D92fs*28, and p.X148_splice), except one sample that harbored a novel frameshift mutation (p.G101fs*39) predicted to be a loss-of-function mutation. All detected mutations in *RB1* were also previously reported pathogenic or likely pathogenic variants (p.V144Lfs*9, p.V222fs*2, p.W99*, p.V450fs*13, p.X500_splice, p.Q597*, and p.E675*).

Comparison of Mutations in SCC In Situ and SCC

Of the most frequently affected genes, mutations in *PIK3CA*, *TP53*, *CDKN2A*, and *RB1* were present in both in situ lesions and invasive carcinomas. The mutations occurred in the same gene locations in both the in situ group and the invasive group. Mutations in *FGFR3*, *JAK3*, and genes involved in epigenetic modulation (the *KMT2* family, *KDM6A*, *CREBBP*, *EP300*, *ATRX*) were predominantly seen in the group of invasive conjunctival SCCs (Supplementary Fig. S2).

Differential Genomic Alterations in HPV-Positive and HPV-Negative Conjunctival SCC

By evaluating the HPV-positive and HPV-negative tumors separately, distinct clusters of mutations were detected. In HPV-positive tumors, mutations of *PIK3CA* were the most common ($n = 5$, 56%). Mutation of *PIK3CA* was also present

in HPV-negative tumors ($n = 3$, 12%) but only co-occurring with mutations in either *TP53* or *RB1* as opposed to HPV-positive tumors. Eighty-eight percent of the HPV-negative tumors harbored mutations in *TP53*, while this was only the case in one HPV-positive tumor (an HPV39-positive SCC in situ). Furthermore, mutations in *CDKN2A* and *RB1* were exclusively present in HPV-negative tumors ($n = 12$, 50%). All samples with *RB1* mutation were positive in p16 IHC. Two HPV-negative cases were positive in p16 IHC but did not harbor an *RB1* mutation.

The phosphatidylinositol-4,5-biphosphate 3-kinase (PI3K) pathway was the most commonly affected pathway in HPV-positive tumors due to alterations in *PIK3CA*, *mTOR*, *TSC1*, and *TSC2*. In HPV-negative tumors, alterations affecting the RTK-RAS pathway (*FGFR3*, *MET*, *NF1*, *FGFR1*, *JAK2*, *NRAS*, *RASA1*, and *RET*) were the most common, followed by the PI3K pathway (*PIK3CA*, *PPP2R1A*, *STK11*, and *TSC2*) and genes related to cell cycle (*CDKN2A* and *RB1*).

Discussion

We present the results of a comprehensive, targeted DNA sequencing of 33 conjunctival SCCs in situ and conjunctival SCCs and for the first time provide insight into two potentially distinct distributions of somatically acquired mutations in conjunctival SCC based on HPV status. We have previously shown differences in clinical and histopathologic features based on HPV status,[1] which, based on the results of the present study, may be grounded in differences on a genomic level.

The HPV-positive SCCs in the present study ($n = 9$; 27%) were characterized by frequent somatic mutations in *PIK3CA*; wild-type *TP53*, *RB1*, and *CDKN2A;* and high-risk HPV transcripts, while pathogenic mutations in *TP53*, *RB1*, and *CDKN2A* characterized the HPV-negative SCCs ($n = 24$; 73%). Both groups had alterations in epigenetic modulators such as members of the KMT2 family, predominantly in the invasive carcinomas.

Notable similarities between in situ lesions and invasive conjunctival SCCs were detected. Alterations in *TP53*, *RB1*, *CDKN2A*, and *PIK3CA* were all consistently identified in both in situ and invasive carcinomas despite HPV status, suggesting that these mutations are events occurring before the invasion of the basal membrane. The acquirement of clonal genomic changes in essential cancer driver genes has been reported in preinvasive conjunctival and cutaneous SCCs[24] and even in morphologically healthy eyelid skin.[25] However, the incidence of mutated *TP53* and *CDKN2A* increases along with the progression of the disease, in accordance with the present study.[24,26]

Due to the important similarities between in situ and invasive conjunctival SCCs, it has previously been suggested that the progression to malignant disease may rely solely on transcriptional or epigenetic events.[24] However, our data suggest that somatic mutations also may contribute to disease progression. We detected differences between in situ and invasive conjunctival SCCs that support a stepwise acquisition of somatic mutations along with the progression of the disease. Mutations in epigenetic modulators, for example, members of the KMT family (*KMT2A*, *KMT2B*, *KMT2C*, *KMT2D*) and *KDM6A*, *CREBBP*, *ATRX*, and *EP300*, were enriched among the invasive conjunctival SCCs—in aggregate, altered in 15 of 25 (60%) SCCs. Chromatin regulators, such as the KMT family, have emerged as a distinct feature of cancer in recent years and are attractive drug targets due to their potential reversibility. These genes have not been assessed previously in conjunctival SCC but are correlated with an aggressive phenotype in SCC of the skin, lung, esophagus, and head and neck and strongly correlate with metastatic spread.[26,27] Furthermore, as HPV relies on an open chromatin landscape to integrate the viral genome into the host genome, dysregulated chromatin regulators may assist HPV integration,[27] which is a critical step in HPV-related carcinogenesis associated with progression from preinvasive to invasive disease.

In HPV-positive conjunctival SCC, we report frequent alterations in *PIK3CA*, *mTOR*, *TSC1*, and *TSC2*, which are predicted to disrupt the PI3K signaling cascade, implicating PI3K pathway activation as central to the carcinogenesis. In combination with the wild-type status of *TP53*, *CDKN2A*, and *RB1*, this points to a distinct way of carcinogenesis compared to HPV-negative conjunctival SCC.

HPV-positive SCCs share mutational profiles across anatomic sites.[28] While some alterations may be due to the direct effect of the HPV, others are caused by the host cell response to the viral infection as well as other potential endogenous (e.g., germline mutations, immune response) or exogenous carcinogens.

Of direct carcinogenic effects provided by HPV, the inactivation of the cell cycle regulators p53 and pRb by the viral oncogenes E6 and E7 is central. This inactivation causes abrogation of cell cycle regulation despite the absence of somatic mutations and can explain the wild-type status of these genes in the HPV-positive SCC. Therefore, regardless of HPV status, the conjunctival SCC development seems to rely on disrupted p53 and/or pRb function, either through genomic alteration or the degradation of the proteins by the HPV oncogenes.

The upregulation of apolipoprotein B mRNA editing catalytic polypeptide-like (APOBEC) cytosine deaminases is an important host cell contribution to HPV-related carcinogenesis. Despite being upregulated to assist viral clearance and reduce the persistence of infection, the APOBEC proteins can contribute to carcinogenesis by inducing somatic mutations. HPV-related carcinomas across sites are enriched of characteristic APOBEC mutations,[29,30] including the characteristic 5′TCW motif mutations of the helical domain in *PIK3CA*,[31] also reported in the present study (Fig. 2c). The enrichment of these mutations is indicative of an APOBEC-induced mutational signature in HPV-positive conjunctival SCC; however, a whole-genome/exome sequencing must be performed to evaluate the mutational signatures of the tumors, but this was outside the scope of the present study.

Not unexpected, loss-of-function mutations in *TP53* were the most frequent mutations in HPV-negative conjunctival SCC, suggesting that abrogation of TP53-dependent pathways is central to the carcinogenesis of these tumors. This pattern correlates well with previous reports of conjunctival SCCs as well as sun-exposed cutaneous SCCs, which report high frequencies of *TP53* somatic mutations, copy number alterations, and aberrant p53 expression.[24,32] Overall, the molecular profile of the HPV-negative tumors of the present study correlates well with the shared mutational profile among SCCs of different anatomic sites, with aberrations in *TP53*, *PIK3CA*, *CDKN2A*, and *FGFR* more often occurring in SCC compared to non-SCC.[33,34]

P16, encoded by *CDKN2A*, indirectly suppresses the phosphorylation of pRb and thereby the cell cycle progression from the G1- to S-phase of mitosis. Deregulation of pRb, for example by genomic alterations or by inactivation of the

Investigative Ophthalmology & Visual Science

HPV oncogene E7, can cause a compensatory increase of p16 expression. In the present study, all *RB1* mutated cases (all HPV negative) overexpressed p16, validating the functional impact of the *RB1* mutations in these cases. Furthermore, a lack of p16 expression was noted in six out of seven samples with mutations in *CDKN2A*. In conclusion, p16 overexpression in the present study was strongly associated with *RB1* mutations or infection with high-risk HPV; meanwhile, most *CDKN2A*-mutated tumors lacked expression of p16.

The present study has several limitations to be considered. First, the cohort size is limited to 33 conjunctival in situ and SCCs, leaving a limited number of samples in each subgroup. This was due to the rarity of the tumor in our latitude combined with the stringent quality controls we applied to ensure high-quality DNA input—potentially inducing selection bias toward larger lesions. Second, the use of FFPE tumor tissue, in some cases stored for >20 years, and the lack of matched germline DNA may have affected the variants called. To compensate, we chose a DNA extraction method and a high-throughput assay specialized for FFPE tissue to reduce artifacts and had stringent criteria in the variant calling to leave out potential germline variations and low-quality calls, well aware that this approach may have overlooked pathogenic low-frequency variants. On the other hand, this setup is readily reproducible in other centers because FFPE is the most common way of preserving tissue, and the availability of matched control tissue often lacks in a clinical setting. Finally, with a targeted sequencing approach, potential aberrations outside the covered areas are not detected, and we limited our study to the investigation of single-nucleotide variants, small insertions, and deletions. We did not evaluate structural variants and copy number variations (CNVs), even though, for example, CNVs of *CDKN2A*, *PTEN*, *FBXW7*, and *SOX2* are frequent in SCC, and this may explain the low mutational rate of these genes in the present study.

Conclusion

In the present study, we have demonstrated different mutational profiles of conjunctival SCCs in situ and SCCs based on HPV status, pointing to distinct biological mechanisms of carcinogenesis. The present study also supports a stepwise acquisition of somatic alterations in the development from preinvasive to invasive disease, with mutations in *TP53*, *RB1*, and *PIK3CA* as early events and mutations of epigenetic modulators such as the KMT gene family as late events.

The shared mutational profile and mechanisms of SCC across different sites, both regarding HPV-positive and HPV-negative carcinomas, have important implications for rare tumors such as conjunctival SCC, in which extensive genomic studies are hard to complete. However, more studies are needed to validate the present findings and further explore the genomic aberrations in conjunctival SCC. Based on the differences between HPV-positive and HPV-negative SCC, we recommend the inclusion of HPV status in future studies of these carcinomas to establish viable biomarkers for this frequently recurrent disease.

Acknowledgments

Supported by the Svend Helge Arvid Schrøder and Ketty Lydia Larsen Schrøder Foundation, Denmark; the Synoptik Foundation, Denmark; "Fight for Sight, Denmark"; Faculty of Health and Medical Science, University of Copenhagen, Denmark; Copenhagen University Hospital, Rigshospitalet; and the Danish Eye Research Foundation. The funding sources had no role in the study design; in the collection, analysis, and interpretation of data; in the writing of the report; or in the decision to submit the article for publication.

Disclosure: **I. Ramberg**, None; **F.G. Vieira**, None; **P.B. Toft**, None; **C. von Buchwald**, None; **M. Funding**, None; **F.C. Nielsen**, None; **S. Heegaard**, None

References

1. Ramberg I, Toft PB, Georgsen JB, et al. Conjunctival intraepithelial neoplasia and carcinoma: distinct clinical and histological features in relation to human papilloma virus status. *Br J Ophthalmol*. 2019;105:878–883.
2. Gichuhi S, Sagoo MS, Weiss HA, Burton MJ. Epidemiology of ocular surface squamous neoplasia in Africa. *Trop Med Int Health*. 2013;18:1424–1443.
3. Cervantes G, Rodríguez AA, Leal AG. Squamous cell carcinoma of the conjunctiva: clinicopathological features in 287 cases. *Can J Ophthalmol*. 2002;37:14–20.
4. Tunc M, Char DH, Crawford B, Miller T. Intraepithelial and invasive squamous cell carcinoma of the conjunctiva: analysis of 60 cases. *Br J Ophthalmol*. 1999;83:98–103.
5. Tabin G, Levin S, Snibson G, Loughnan M, Taylor H. Late recurrences and the necessity for long-term follow-up in corneal and conjunctival intraepithelial neoplasia. *Ophthalmology*. 1997;104:485–492.
6. Galor A, Karp CL, Oellers P, et al. Predictors of ocular surface squamous neoplasia recurrence after excisional surgery. *Ophthalmology*. 2012;119:1974–1981.
7. Abt NB, Zhao J, Huang Y, Eghrari AO. Prognostic factors and survival for malignant conjunctival melanoma and squamous cell carcinoma over four decades. *Am J Otolaryngol*. 2019;40:577–582.
8. Galor A, Karp CL, Chhabra S, Barnes S, Alfonso EC. Topical interferon alpha 2b eye-drops for treatment of ocular surface squamous neoplasia: a dose comparison study. *Br J Ophthalmol*. 2010;94:551–554.
9. Venkateswaran N, Mercado C, Galor A, Karp CL. Comparison of topical 5-fluorouracil and interferon alfa-2b as primary treatment modalities for ocular surface squamous neoplasia. *Am J Ophthalmol*. 2019;199:216–222.
10. Parrozzani R, Frizziero L, Trainiti S, et al. Topical 1% 5-fluoruracil as a sole treatment of corneoconjunctival ocular surface squamous neoplasia: long-term study. *Br J Ophthalmol*. 2017;101:1094–1099.
11. Ramberg I, Møller-Hansen M, Toft PB, Funding M, Heegaard S. Human papillomavirus infection plays a role in conjunctival squamous cell carcinoma: a systematic review and meta-analysis of observational studies. *Acta Ophthalmol*. 2021;99:478–488.
12. Loyo M, Li RJ, Bettegowda C, et al. Lessons learned from next-generation sequencing in head and neck cancer. *Head Neck*. 2013;35:454–463.
13. Grønhøj C, Jensen DH, Agander T, et al. Deep sequencing of human papillomavirus positive loco-regionally advanced oropharyngeal squamous cell carcinomas reveals novel mutational signature. *BMC Cancer*. 2018;18:640.
14. Bjerregaard B, Larsen OB. The Danish Pathology Register. *Scand J Public Health*. 2011;39:72–74.
15. Amin MB, Greene F , et al., eds. *AJCC Cancer Staging Manual*. 8th ed. New York, NY: Springer; 2017.
16. Do H, Wong SQ, Li J, Dobrovic A. Reducing sequence artifacts in amplicon-based massively parallel sequencing of formalin-fixed paraffin-embedded DNA by enzymatic

depletion of uracil-containing templates. *Clin Chem*. 2013;59:1376–1383.
17. Andrew S. FastQC: a quality control tool for high throughput sequence data. 2010, http://www.bioinformatics.babraham.ac.uk/projects/fastqc. Accessed April 10, 2021.
18. Pedersen BS, Quinlan AR. Mosdepth: quick coverage calculation for genomes and exomes. *Bioinformatics*. 2018;34:867–868.
19. Van der Auwera GA, O'Connor BD. *Genomics in the Cloud: Using Docker, GATK, and WDL in Terra*. O'Reilly Media:Sebastopol, CA, USA; 2020.
20. Karczewski KJ, Francioli LC, Tiao G, et al. The mutational constraint spectrum quantified from variation in 141,456 humans. *Nature*. 2020;581:434–443.
21. Cerami E, Gao J, Dogrusoz U, et al. The cBio cancer genomics portal: an open platform for exploring multidimensional cancer genomics data. *Cancer Discov*. 2012;2:401–404.
22. Gao J, Aksoy BA, Dogrusoz U, et al. Integrative analysis of complex cancer genomics and clinical profiles using the cBioPortal. *Sci Signal*. 2013;6:pl1.
23. Mayakonda A, Lin DC, Assenov Y, Plass C, Koeffler HP. Maftools: efficient and comprehensive analysis of somatic variants in cancer. *Genome Res*. 2018;28:1747–1756.
24. Lazo de la Vega L, Bick N, Hu K, et al. Invasive squamous cell carcinomas and precursor lesions on UV-exposed epithelia demonstrate concordant genomic complexity in driver genes. *Mod Pathol*. 2020;33:2280–2294.
25. Martincorena I, Roshan A, Gerstung M, et al. Tumor evolution. High burden and pervasive positive selection of somatic mutations in normal human skin. *Science*. 2015;348:880–886.
26. Yilmaz AS, Ozer HG, Gillespie JL, et al. Differential mutation frequencies in metastatic cutaneous squamous cell carcinomas versus primary tumors. *Cancer*. 2017;123:1184–1193.
27. Haft S, Ren S, Xu G, et al. Mutation of chromatin regulators and focal hotspot alterations characterize human papillomavirus-positive oropharyngeal squamous cell carcinoma. *Cancer*. 2019;125:2423–2434.
28. Litwin TR, Clarke MA, Dean M, Wentzensen N. Somatic host cell alterations in HPV carcinogenesis. *Viruses*. 2017;9:206.
29. The Cancer Genome Atlas Research Network. Integrated genomic and molecular characterization of cervical cancer. *Nature*. 2017;543:378–384.
30. Henderson S, Chakravarthy A, Fenton T. When defense turns into attack: antiviral cytidine deaminases linked to somatic mutagenesis in HPV-associated cancer. *Mol Cell Oncol*. 2014;1:e29914.
31. Henderson S, Chakravarthy A, Su X, Boshoff C, Fenton TR. APOBEC-mediated cytosine deamination links PIK3CA helical domain mutations to human papillomavirus-driven tumor development. *Cell Rep*. 2014;7:1833–1841.
32. Ateenyi-Agaba C, Dai M, Le Calvez F, et al. TP53 mutations in squamous-cell carcinomas of the conjunctiva: evidence for UV-induced mutagenesis. *Mutagenesis*. 2004;19:399–401.
33. Schwaederle M, Elkin SK, Tomson BN, Carter JL, Kurzrock R. Squamousness: next-generation sequencing reveals shared molecular features across squamous tumor types. *Cell Cycle*. 2015;14:2355–2361.
34. Dotto GP, Rustgi AK. Squamous cell cancers: a unified perspective on biology and genetics. *Cancer Cell*. 2016;29:622–637.

Investigative Ophthalmology & Visual Science